

AD-A151 358 NF(B SUPERSCRIPT 1 SIGMA +) FROM DISCHARGE-INITIATED
NF(A1 DELTA) AND CHE. (U) DEFENCE RESEARCH
ESTABLISHMENT VALCARTIER (QUEBEC) S A BARTON ET AL.
SEP 84 DREV-4344/84

1/1

UNCLASSIFIED

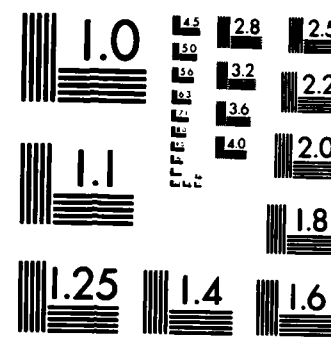
F/G 7/4

NL

END

FILMED

OTIC



MICROCOPY RESOLUTION TEST CHART
NATIONAL BUREAU OF STANDARDS-1963-A



National
Defence

Defense
nationale

REPRODUCED AT GOVERNMENT EXPENSE

UNCLASSIFIED
UNLIMITED DISTRIBUTION

2

DREV REPORT 4344/84
FILE: 3633H-007
SEPTEMBER 1984

CRDV RAPPORT 4344/84
DOSSIER: 3633H-007
SEPTEMBRE 1984

AD-A151 358

NF($b^1\Sigma$) FROM DISCHARGE-INITIATED NF($a^1\Delta$)
AND CHEMICAL O₂($a^1\Delta g$)

S.A. Barton

K.D. Foster

V. Lettau

DTIC
ELECTED
MAR 18 1985
S D
B

DTIC FILE COPY

DISTRIBUTION STATEMENT A
Approved for public release
Distribution Unlimited

Centre de Recherches pour la Défense

Defence Research Establishment

Valcartier, Québec

BUREAU RECHERCHE ET DÉVELOPPEMENT
MINISTÈRE DE LA DÉFENSE NATIONALE
CANADA

RESEARCH AND DEVELOPMENT BRANCH
DEPARTMENT OF NATIONAL DEFENCE
CANADA

Canada

NON CLASSIFIÉ
DIFFUSION ILLIMITÉE

84 11 14 032

DREV R-4344/84
FILE: 3633H-007

UNCLASSIFIED

CRDV R-4344/84
DOSSIER: 3633H-007

**NF($b^1\Sigma^+$) FROM DISCHARGE-INITIATED NF($a^1\Delta$) AND
CHEMICAL O₂($a^1\Delta g$)**

by

S.A. Barton and K.D. Foster

CENTRE DE RECHERCHES POUR LA DÉFENSE

DEFENCE RESEARCH ESTABLISHMENT

VALCARTIER

Tel: (418) 844-4271

Québec, Canada

September/septembre 1984

NON CLASSIFIÉ

UNCLASSIFIED

1

ABSTRACT

Chemically generated $O_2(a^1\Delta g)$ was used to excite $NF(a^1\Delta)$ to $NF(b^1\Sigma^+)$ in a vacuum flow system, $NF(a)$ being produced by the reaction of discharge-generated D atoms with NF_2 radicals. Maximum concentrations of the $NF(a)$ and b states were 5×10^{14} and 7×10^{12} cm^{-3} respectively. The latter value is too low to support a blue-green laser based on $NF(b^1\Sigma^+)$.

A complex kinetic model was developed involving 14 known elementary reactions. Using our experimental conditions as input, the coupled rate equations from this model were numerically integrated to yield rate constants for the forward and reverse $O_2(a) + NF(a)$ reaction (6.7 and 1.3×10^{-14} cm^3 molecule $^{-1}$ s^{-1} respectively), and for the quenching of $NF(a)$ and $NF(b)$ by H_2O vapour (4 and 5×10^{-13} cm^3 molecule $^{-1}$ s^{-1} respectively).

The kinetic model shows that a very fast reaction from $NF(a)$ to $NF(b)$ is required in order to achieve a population inversion between $NF(b)$ and the ground state $NF(X)$. Excited atomic iodine, $I(^2P_1)$, appears to be a better candidate than $O_2(a^1\Delta g)$ for generating high densities of $NF(b)$.

Nitrogen fluoride (a superscript 1 segment)

Accession For	
NTIS CRA&I	<input checked="" type="checkbox"/>
DTIC TAB	<input type="checkbox"/>
Unpublished	<input type="checkbox"/>
Justification	
By _____	
Distribution/	
Availability Codes	
Dist	Avail and/or Special
A-1	



RÉSUMÉ

Du $O_2(a^1\Delta g)$ généré chimiquement a été utilisé pour exciter le $NF(a^1\Delta)$ à $NF(b^1\Sigma^+)$ dans un système d'écoulement sous vide. Du $NF(a)$ a alors été formé par la réaction engendrée par une décharge d'atomes D avec des radicaux NF_2 . Les concentrations maximales de NF déterminées dans les états a et b sont respectivement 5×10^{14} et $7 \times 10^{12} \text{ cm}^{-3}$. Cette dernière concentration est trop faible pour supporter une action laser basée sur le $NF(b^1\Sigma^+)$ dans la région bleu-vert.

Un modèle cinétique complexe a été développé impliquant 14 réactions élémentaires connues. En utilisant nos valeurs expérimentales, les équations de vitesse couplées ont été intégrées numériquement afin de fournir les constantes de vitesse de la réaction $O_2(a) + NF(a)$ dans les deux directions (6.7×10^{-14} et $1.3 \times 10^{-14} \text{ cm}^3 \text{ molécule}^{-1} \text{ s}^{-1}$ pour la réaction inverse). Les constantes de vitesse de la désactivation de $NF(a)$ et $NF(b)$ par H_2O ont aussi été calculées (4 et $5 \times 10^{-13} \text{ cm}^3 \text{ molécule}^{-1} \text{ s}^{-1}$ respectivement).

Le modèle cinétique montre qu'il faudrait une excitation très rapide de $NF(a)$ à $NF(b)$ afin de réaliser une inversion de population entre $NF(b)$ et l'état fondamental $NF(X)$. L'iode atomique excité $I(^2P_1)$ semble être un meilleur candidat que le $O_2(a^1\Delta g)$ pour générer de fortes densités de $NF(b)$.

UNCLASSIFIED

iii

TABLE OF CONTENTS

ABSTRACT.	1
RESUME	ii
1.0 INTRODUCTION	1
2.0 EXPERIMENTAL	3
2.1 Apparatus and Reagents	3
2.2 Concentration Estimates from Emission Measurements	6
2.3 Results.	7
3.0 KINETIC MODELLING	13
3.1 Generation of NF($a^1\Delta$).	13
3.2 Generation of NF($b^1\Sigma^+$)	16
3.3 Accuracy of Rate Constants	20
3.4 Rapid Pumping of NF($a^1\Delta$) for $b^1\Sigma^+$ Population Inversion .	21
4.0 CONCLUSIONS	22
5.0 ACKNOWLEDGEMENTS	23
6.0 REFERENCES	24

TABLES I to III

FIGURES 1 to 6

UNCLASSIFIED

1

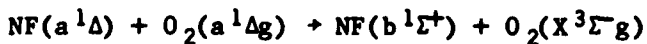
1.0 INTRODUCTION

The second electronically excited state of nitrogen fluoride emits spontaneously in a band around 529 nm: the 0-0 band of the $b^1\Sigma^+$ - $X^3\Sigma^-$ system. This emission is in the blue-green region of the spectrum, which is suitable for transmission through ocean water. The development of lasers in this wavelength region is of interest to DND for use in airborne bathymetry and the detection of submarines, torpedoes, and mines.

A gain medium for a laser based on gaseous nitrogen fluoride would require $NF(b^1\Sigma^+)$ in concentrations greater than any ground state $NF(X^3\Sigma^-)$ that is present, and sufficiently high to ensure reasonable gain over a practical path length. We have estimated (Ref. 1) that for a 5% gain over 2 m, a number density difference between the two states of greater than 10^{15} molecules cm^{-3} would be necessary. This high concentration requirement is largely due to the long radiative lifetime (23 ms; Ref. 2) of $NF(b^1\Sigma^+)$.

It has been shown (Refs. 3-9) that NF is produced almost exclusively in the first electronically excited state ($a^1\Delta$) by the gas phase reaction of hydrogen or deuterium atoms with the difluoroamino radical NF_2 . Maximum concentrations in the region of 10^{15} cm^{-3} have been reported (Ref. 7), where a high-voltage electrical discharge was used to produce D or H by first generating F atoms in a mixture of SF_6 and D_2 or H_2 .

$NF(a^1\Delta)$ may be further excited to the $b^1\Sigma^+$ state by a reaction with singlet delta oxygen (Refs. 2, 6, 10):



+ 415 cm^{-1}

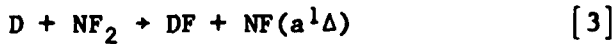
[1]

This is an electronic energy-pooling process, similar to that in $O_2(a^1\Delta g)$ itself. The second-order rate constant has not previously been well established, although the process was believed to be rather slow ($\sim 10^{-14} \text{ cm}^3 \text{ molecule}^{-1} \text{ s}^{-1}$; Ref. 4). This rate, the reverse reaction rate, and the relevant quenching rates of the excited a and b states of NF are crucial in determining the feasibility of reaction [1] to drive an NF(b) laser, and are discussed in detail in Chapters 3.0 and 4.0.

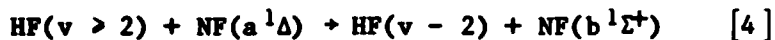
With the development of the chemical oxygen-iodine laser, an entirely chemical method for generating highly concentrated $O_2(a^1\Delta g)$ was introduced (Refs. 11-15). Number densities in excess of 10^{16} cm^{-3} are readily attainable.

We have built a chemical oxygen generator at DREV. Its construction, operation and output have been described elsewhere (Ref. 16). For the flow systems described in this report, the generator supplied about 25% $O_2(a^1\Delta g)$ in a total O_2 pressure of about 1 torr to a downstream reaction cavity.

This report (Chapter 2.0) describes the generation and measurement of NF(b) by the reaction of chemically produced $O_2(a)$ with NF(a). The latter was formed in gas mixtures subjected to either high-voltage or microwave discharge initiation. In both cases, the discharge energy produced F atoms to initiate the reactions:



D_2 was used rather than H_2 for two reasons. Firstly, we wished to study the generation of NF(b) from reaction [1] without interference from the vibrational-electronic energy transfer that can occur in the presence of vibrationally excited HF (Refs. 4, 6, 7, 17):



This occurs because there is a close matching between the energies of two vibrational quanta in HF and the NF a-b electronic transition (0-0 band). The green NF(b) emission is observed in discharge-initiated H₂/NF₂ mixtures, whereas with D₂ it is not, because the DF vibrational spacings are different. Secondly, in the presence of excess ground state HF, the reverse of reaction [4] could lead to a rapid quenching of NF(b).

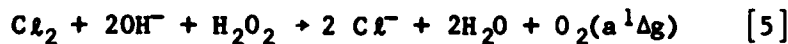
In Chapter 3.0, a kinetic model is presented that involves 14 known elementary reactions, and the coupled differential equations defining the time evolution of the species concentrations are integrated numerically from the initial conditions of our experiments. By comparing calculated measurements with experimental ones for NF(b,a) and O₂(a) concentrations, we infer rate constants for reaction [1] and the quenching of the a and b states of NF by water vapour, which is present in the flow from the O₂(a) generator.

This work was performed at DREV between June 1981 and March 1983 under PCN 33H07, Research on Chemically Excited Lasers.

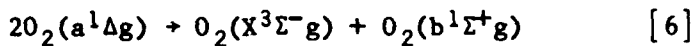
2.0 EXPERIMENTAL

2.1 Apparatus and Reagents

Reference 16 describes the vacuum flow system used to generate O₂(a). The heterogeneous gas-liquid phase reaction involves bubbling Cl₂ through a cooled aqueous alkaline solution of hydrogen peroxide. The overall reaction is the following:



The oxygen that leaves the liquid is close to 100% in the $^1\Delta$ state, and the chlorine conversion efficiency is also almost 100%. In the flow from the liquid surface to a downstream reaction cavity, the major decay mechanisms are energy pooling (cf. reaction [1]):



wall collisions, and quenching by solution vapour and entrained droplets (Ref. 16). Radiative losses (Refs. 18, 19) are insignificant in the time domain (< 0.5 s) for transport in our system. At the reaction chamber, about 25% of the oxygen is in the $O_2(^1\Delta)$ state.

Our results show (Section 2.3) that water vapour is a significant quencher of the excited states of NF. However, its removal presents other problems: cold traps may become blocked with ice, and at coolant temperatures lower than -80°C , significant deactivation of $O_2(a)$ could occur (Ref. 14). Ethanol/dry ice is a suitable coolant for a trap between the generator and reaction zone.

Tetrafluorohydrazine (Air Products Inc.) was used, without further purification, as a source of NF_2 . It readily dissociates when warmed:



For example, mixtures at pressures up to 0.5 torr are greater than 80% NF_2 at 100°C . The extent of dissociation increases with increasing temperature and decreasing pressure (Ref. 20). The equilibrium [7] is reached rapidly (Refs. 21, 22) within the flow times expected here.

Figure 1 shows the two reaction vessels that we have used for the discharge-initiated generation of NF. The upper diagram shows a Pyrex reactor that had four microwave cavities attached to separate 13-mm inlet tubes. These inlets converged to a single outlet orifice

UNCLASSIFIED

5

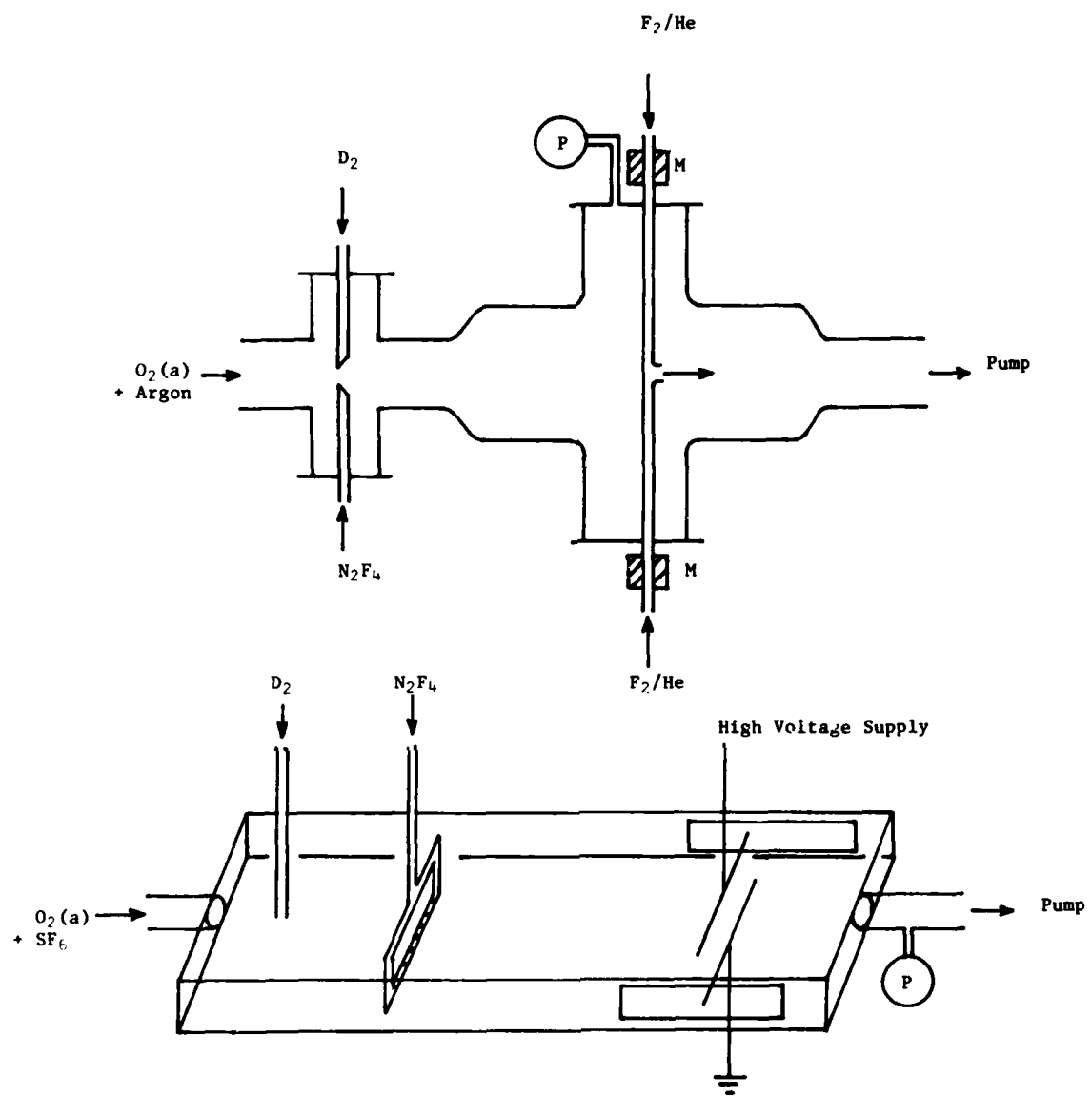


FIGURE 1 - Microwave and high-voltage discharge reaction vessels
(M - microwave cavity; P - pressure gauge)

at the centre of a cross. The microwave generators were operated at 2450 MHz and 100 W, with < 5 W reflected power. D_2 , N_2F_4 and O_2 were premixed in a 2.5-cm-diameter section about 15 cm before the main reaction zone, which was in a 5-cm-diameter tube immediately downstream of the microwave discharged F_2 inlet.

The high-voltage discharge cell of Fig. 1 was made of Perspex coated internally with Teflon. It was of rectangular cross section (1 x 12 cm) and about 30 cm long. Removable Supracil II windows were used to view the high-voltage discharge region. The electrodes were 1-cm-wide aluminum strips 10 cm in length, 9 cm of which were covered with Teflon so that only the diagonally opposite ends remained exposed. Operating in the 20-25 kV range, a 500 pF capacitor produced a discharge pulse of less than 2- μ s duration. A uniform glow was obtained over the entire $\sim 10 \text{ cm}^3$ volume of the discharge region, without arcing, in SF_6 /argon mixtures in the 5-15 torr pressure range. The N_2F_4 inlet was designed to provide a uniform gas flow across the cavity. It was a 0.125-in diameter copper tube pierced with 20 holes of diameter ~ 0.5 mm. SF_6 was premixed with the Cl_2 and passed through the $O_2(a^1\Delta g)$ generator solution. This did not affect the performance of the generator (Ref. 16).

In both discharge systems, the N_2F_4 inlets were wrapped with heating tape capable of attaining 200°C. Pressures were measured with capacitance manometers (MKS and Vacuum General) and mass flow rates with Hastings and Vacuum General meters.

2.2 Concentration Estimates from Emission Measurements

Transitions to the NF ground state from the $a^1\Delta$ and $b^1\Sigma^+$ states give spontaneous emission in bands around 874 nm and 529 nm respectively. We have quantitatively measured the excited species using narrow-band interference filters (10 nm FWHM, blocking < 10^{-6} from UV to 2 μ m) and an HUV 4000B EG&G silicon detector. The detector/filter

combinations were calibrated absolutely using an NBS certified quartz-iodine lamp. Detector voltages were measured with a digital voltmeter.

The detailed calculation of species concentrations from absolute emission measurements on an extended source has been described previously (Ref. 23). A focusing lens ($f = 6.4$ cm) and 1-cm-diameter circular aperture were used to define contributing volumes in the HV and microwave vessels respectively. The calculations account in detail for the extended nature of the emission by performing a numerical integration over the contributing volume. Apart from physical dimensions, the required input parameters are: the detector calibration constant at the emission wavelength; the measured detector voltage; a transmission factor for the interference filter (see Appendix A of Ref. 16); and the spontaneous emission radiative rate constant (κ_s). With carefully measured distances and detector calibrations, the method can give species concentrations within 20% error limits if κ_s is known to within 10%. This is the case for the $a^1\Delta$ and $b^1\Sigma^+$ states of NF (Refs. 2, 9). Relative detector voltages from our experimental microwave discharge-initiated NF emissions were recorded using a chopper/lock-in amplifier setup, and placed on an absolute basis using the same digital voltmeter that was used in the detector calibration. NF emissions from the HV cell were recorded directly as voltages on an oscilloscope.

2.3 Results

The behaviour of a mixture of D_2 (or H_2) and N_2F_4 is very sensitive to the temperature and partial pressures of the components. In a static system at $90^\circ C$, H_2 and N_2F_4 form explosive mixtures (Ref. 24) in molar ratios of 2:1, 1:1 and 1:2 at total pressures of 6 torr. The initiation step is thought to involve H_2 and NF_2 . This step is endothermic, but subsequent reactions are highly exothermic. In flow systems, self-sustaining emissions from NF and excited N_2 have been observed in discharge-initiated mixtures (Refs. 25, 26).

We have confirmed this flow system behaviour. Over a range of pressures up to 6 torr, with molar ratios varying from 1:1 to 8:1 (D_2 : N_2F_4), it is possible to generate a continuous intense yellow emission at the gas inlets using microwave, Tesla coil, or pulsed high-voltage initiation. This yellow light arises from the $B^3\Pi_g$ - $A^3\Sigma_u$ system of N_2 (Refs. 3, 8, 25). If the inlet tubes become hot ($> \sim 100^\circ C$), the reaction may occur without discharge initiation. At lower partial pressures (~ 1 torr each), we have found it possible to suppress this spontaneous D_2/N_2F_4 combustion with argon flowing at up to 1500 SCCM. This is desirable because a much weaker green emission is observed with $O_2(a)$ if the D_2/N_2F_4 combustion occurs before the F atom reaction zone (Fig. 1). At pressures above about 1 torr each of D_2 and N_2F_4 , the combustion is difficult to prevent.

We have also observed a self-sustaining green emission from $NF(b)$ in discharge-initiated mixtures of D_2 , N_2F_4 and $O_2(a)$.

The following two subsections summarize our optimized experimental conditions and measured NF (a and b) concentrations obtained in the microwave and HV discharge vessels respectively.

2.3.1 Microwave Discharge Initiation

Up to 80% dissociation of F_2 can be achieved by microwave discharge of a helium-diluted gas flow in the 1-2 torr pressure range (Ref. 27). We have used a 2% F_2 in He mixture (Matheson Gas Products) at pressures between 1 and 3 torr. Maximum F atom densities in the region of 10^{15} cm^{-3} could therefore be expected.

Optimum partial pressures of the reacting gases are given in column 2 of Table I. These were obtained by maximizing the detector signal using a 529-nm interference filter, i.e. $NF(b)$ emission.

UNCLASSIFIED

9

TABLE I
Optimized partial pressures

Gas	Partial Pressure (torr)	
	Microwave	High Voltage
2ZF_2 in He	2.40	-
SF_6	-	8.50
D_2	0.30	1.20
NF_2	0.25	0.40
O_2	0.90	1.10
H_2O (a)	0.90-1.20	1.40
H_2O (b)	0.4-0.5	-

(a) no cold trap; (b) dry ice/ethanol trap

The pressure listed for NF_2 is the change observed when the N_2F_4 flow was turned on and off: at 100°C, the approximate cavity temperature, a measured total pressure of 0.25 torr in a $\text{N}_2\text{F}_4/\text{NF}_2$ mixture is 90% NF_2 (Ref. 20). Similarly, the O_2 pressure is the change measured when the Cl_2 flow through the generator was turned on and off. About 25% of this total O_2 was $\text{O}_2(\text{a}^1\Delta\text{g})$, i.e. a density of $\sim 6 \times 10^{15} \text{ cm}^{-3}$ at 100°C. Table I also shows the H_2O vapour pressures measured in the cavity with and without a dry ice/ethanol coolant in the trap at the outlet of the O_2 generator. The lower pressures in each case were obtained with the generator solution at -14°C. During the reaction with Cl_2 , the solution warmed to $\sim -10^\circ\text{C}$, for which the upper values of H_2O pressure are applicable.

With the partial pressures given in column 2 of Table I and no cold trap, we measured NF concentrations in five separate experiments. Our values lay in the ranges:

UNCLASSIFIED

10

$$[NF(b)] = (2.6 - 4.0) \times 10^{12} \text{ cm}^{-3}$$

[8]

$$[NF(a)] = (1.5 - 3.5) \times 10^{14} \text{ cm}^{-3}$$

with $[H_2O] \sim 1$ torr.

The factor of 100 between the concentrations of the two species is quite consistent. In Chapter 3.0, this is shown to be a key relationship in our estimate of the rate of reaction [1].

The condition of the Pyrex glassware is important. The upper values of the ranges in [8] were obtained when the reactor walls and F atom inlet tubes had been freshly rinsed with a 10% aqueous solution of HF, and dried by pumping down to ~ 0.01 torr.

When H_2 was used in place of D_2 , an approximately 19% reduction in $NF(b)$ emission was observed.

The removal of H_2O vapour from the O_2 gas stream also has a significant effect. A dry ice/ethanol cold trap reduced the H_2O pressure from ~ 1 to 0.45 torr (Table I). This decrease results in a consistent increase in $[NF(b)]$ by a factor of 1.7 (an average of 3 experimental values: 1.75, 1.68, 1.58). A similar 1.5-fold increase in $[NF(a)]$ was recorded when H_2O was reduced from 1 to 0.1 torr using liquid nitrogen as trap coolant.

With an ethanol/dry ice trap, the maximum $[NF(b)]$ recorded was:

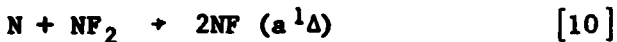
$$[NF(b)]_{max} = 6.7 \times 10^{12} \text{ cm}^{-3}$$

[9]

with $[H_2O] \sim 0.45$ torr.

We have also investigated the dependence of NF(b) emission intensity on the gas mixture used in the discharge. Small amounts of NF_3 or SF_6 were premixed with the 2% F_2/He stream in an attempt to increase the F atom yield. NF(b) emission intensities simply decreased with increasing additive flow. Apparently, F_2 is more easily dissociated in a microwave discharge than NF_3 or SF_6 (the F-F bond strength is less than that of N-F or S-F in these molecules).

Pure N_2 was also discharged in an attempt to replace reactions [2] and [3] by the single step:



In this experiment, neither D_2 nor F_2/He was employed. However, much less NF(b) was produced ($< 10^{11} \text{ cm}^{-3}$).

F_2 diluted in helium was the most effective mixture for the microwave discharge-initiated production of NF(b).

There was clear evidence that the concentration of NF(b) depended on the density of F atoms introduced into the reaction mixture. When the power to each of the four microwave cavities was turned off sequentially, we observed a proportionate reduction in NF(b) emission in the region immediately after the F_2 inlet; i.e. a detector voltage of 1.00 with 4 operating discharges would be reduced to about 0.75, 0.50 and 0.25 with 3, 2 and 1 discharges respectively.

There was also evidence of a direct reaction between D_2 and NF_2 when the flow system had become quite hot ($\sim 80^\circ\text{C}$). Reference 24 postulates this endothermic reaction as the initiator in the explosive reaction between D_2 or H_2 and N_2F_4 . When all four discharges were turned off, there remained a continuous self-sustained green emission throughout the flow system, but with low intensity ($\text{NF(b)} \sim 10^{11} \text{ cm}^{-3}$).

We also observed weak green emission ($NF(b) < 10^{11} \text{ cm}^{-3}$) when F atoms were in the presence of D_2 and NF_2 alone, i.e. in the absence of $O_2(a^1\Delta g)$.

2.3.2 High-Voltage Discharge Initiation

With the high-voltage (HV) discharge conditions described in Section 2.1, we recorded $NF(b)$ emission from the cell of Fig. 1 as voltage traces on an oscilloscope, the x-axis being time from the HV trigger pulse. Thus we were able to follow the time evolution of the $NF(b)$ concentration from an essentially instantaneous atom-producing initiation step.

We obtained maximum $NF(b)$ densities similar to those of the microwave discharge experiments. The gas pressures listed in column 3 of Table I produced

$$[NF(b)]_{\text{max}} = 2.7 \times 10^{12} \text{ cm}^{-3} \quad [11]$$

with $[H_2O] \sim 1.4 \text{ torr}$ (no trap coolant).

Figure 2 shows experimental points, drawn as circles, taken from a typical oscilloscope trace. The solid line through these points is a theoretical curve generated by the model described in Chapter 3.0. It is significant that the approximate rise time ($< 100 \mu\text{s}$) of the experimental $NF(b)$ signal is reproduced by the kinetic model.

A series of HV-discharge experiments showed no measurable $NF(b)$ emission in the absence of $O_2(a^1\Delta g)$, indicating that reaction [1] was indeed the mechanism for $NF(b)$ generation.

We were unable to increase $NF(b)$ emission by increasing the discharge energy (500, 1000, and 1500 pF capacitors) and increasing the SF_6 partial pressure, because the discharge began to arc. Similarly,

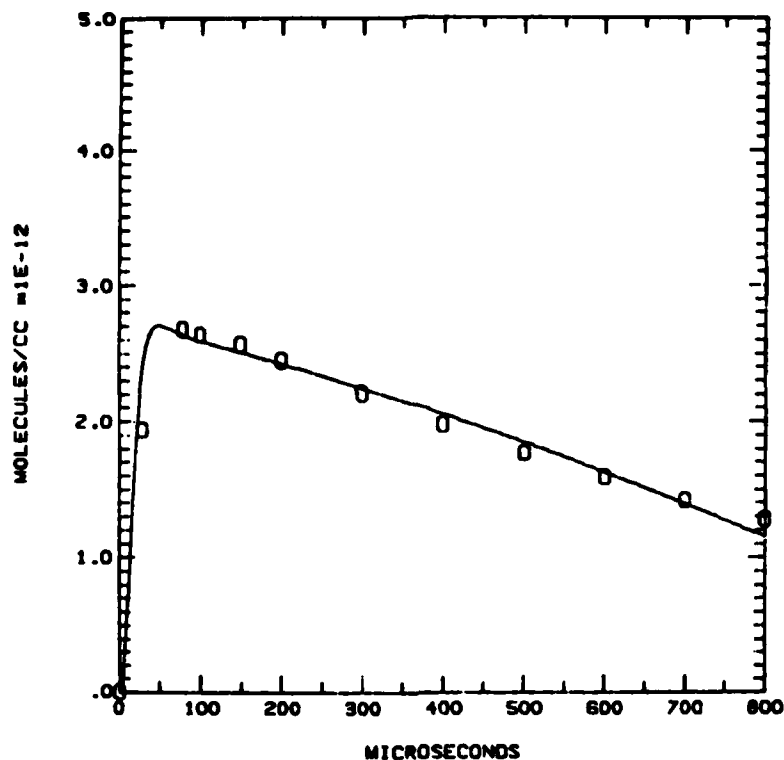


FIGURE 2 - NF(b) from high-voltage discharge

variation of the gas pressures and components (NF₃ was used in place of N₂F₄, and H₂ replaced D₂) led to no increase in NF(b) emission.

3.0 KINETIC MODELLING

3.1 Generation of NF(a¹Δ)

The complex reaction system initiated by H or D atoms in the presence of NF₂ has been extensively studied (Refs. 3-10, 17, 24-28). Table II shows the known elementary reaction steps, i.e. with no intermediate products, that are fast enough to be of consequence in our generation of NF(a).

UNCLASSIFIED

14

Reactions (i) and (ii) are the well-known atom reactions in D_2/F_2 mixtures. With F atoms being produced in our experimental discharge schemes, reaction (i) is the initiation step for the entire system. Reaction (iii) is the principal generator of $NF(a)$, and the quenching processes (vii) to (ix) are the main channels for its removal. Reaction (x), a rapid bimolecular disproportionation, leads to a sustained generation of $NF(a)$ by recycling F atoms through reaction (i), and is a mechanism for the removal of ground state NF.

TABLE II

Generation of $NF(a^1\Delta)$

Reaction	Product	Rate Constant (cm^3 molecule $^{-1}$ s $^{-1}$)	Reference No.
(i) $F + D_2$	$DF + D$	$k_1 = 1.4 \times 10^{-11}$	29,30
(ii) $D + F_2$	$DF + F$	$k_2 = 2.0 \times 10^{-12}$	31
(iii) $D + NF_2$	$DF + NF(a)$	$k_3 = 1.2 \times 10^{-11}$	28
(iv) $D + NF(a)$	$DF + N$	$k_4 = 2.0 \times 10^{-13}$	8,25
(v) $N + NF(a)$	$N_2 + F$	$k_5 = 3.0 \times 10^{-11}$	8
(vi) $N + NF_2$	$2NF(a)$	$k_6 = 3.0 \times 10^{-12}$	25,28
Quenching:			
(vii) $NF(a) + NF_2$	$NF(X) + NF_2$	$k_7 = 2.1 \times 10^{-12}$	28
(viii) $NF(a) + DF$	$NF(X) + DF$	$k_8 \sim 1 \times 10^{-13}$	6,28
(ix) $NF(a) + H_2O$	$NF(X) + H_2O$	$k_9 = 3.7 \times 10^{-13}$	This work
Disproportionation:			
(x) $2NF(X)$	$N_2 + 2F$	$k_{10} = 7.0 \times 10^{-11}$	25

Of the rate constants given in Table II, only that for the quenching of NF(a) by H₂O (k_9) has not been measured elsewhere. The quenching rate due to DF (k_8) was assumed similar to those for HF, HCl and HBr (Refs. 6, 28). This is discussed further in Section 3.3. We have estimated the H₂O quenching rate from our measurements of [NF(a)] generated in different H₂O pressures (Subsection 2.3.1). The calculation is described in the next paragraph.

Among the initial reactants of Table II, i.e. F, D₂, F₂, NF₂, and H₂O, only the F atom concentration was not known from partial pressure measurements. Given an initial guess for F and an H₂O quenching constant k_9 , we have numerically solved the coupled first-order rate equations for all the components of the system using our generalized kinetics FORTRAN program (Ref. 32). In particular, time profiles of [NF(a)] have been generated for the period (2 ms) which we estimate our detection system was viewing, i.e. time averaging, for the continuous microwave discharge experiments. By varying initial [F] and k_9 iteratively, we were able to reproduce our experimental NF(a) concentrations (averaged over 2 ms) measured in 1 and 0.1 torr of H₂O vapour.

Figure 3 shows the results of these calculations. The lower curve is the time profile of [NF(a)] in 1 torr H₂O, with an average value of $3.5 \times 10^{14} \text{ cm}^{-3}$, while the upper curve shows a 1.5-fold increase in average value with 0.1 torr H₂O (cf. Subsection 2.3.1). These calculations indicate an initial [F] of $1.1 \times 10^{15} \text{ cm}^{-3}$, or about 40% dissociation of F₂ from the microwave discharge. The value of k_9 is given in Table II. The two fit parameters are completely independent.

The initial peaks in the curves of Fig. 3 demonstrate the rapid initial generation of NF(a), followed by rapid quenching, and then recycling by reaction (x) of Table II, which becomes significant as [NF(X)] grows.

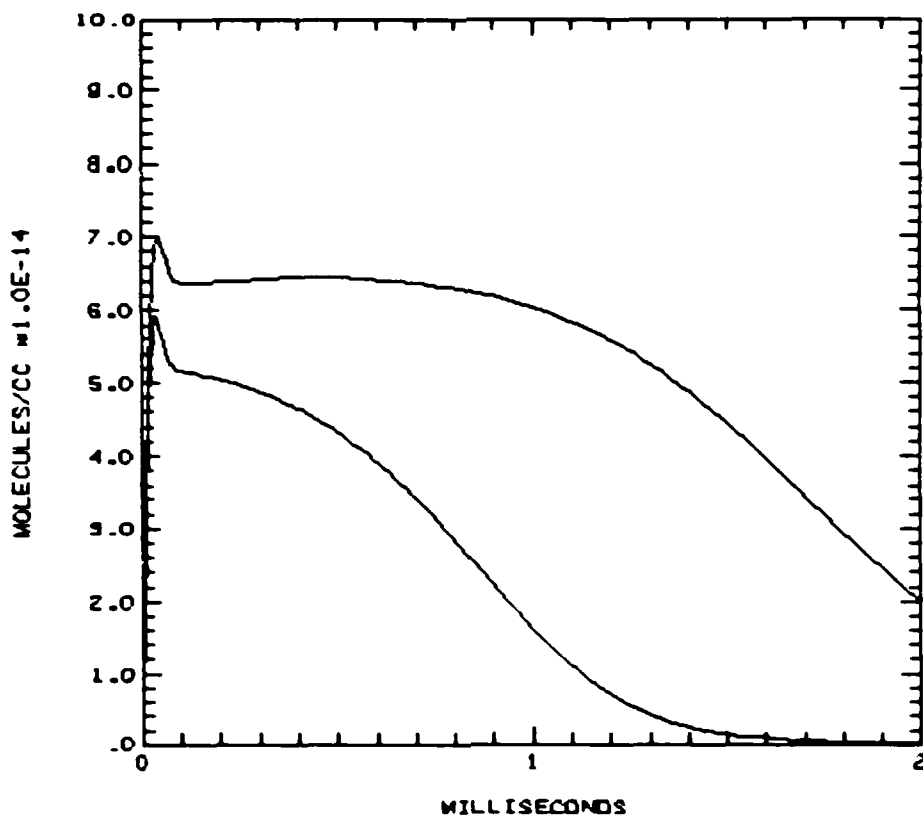


FIGURE 3 - Effect of H_2O on $\text{NF}(\text{a})$ generation

3.2 Generation of $\text{NF}(\text{b}^1\Sigma^+)$

Table III shows the significant additional reactions that can occur when $\text{O}_2(\text{a}^1\Delta\text{g})$ is introduced into the $\text{NF}(\text{a})$ generation scheme of Table II.

Initial concentrations of $\text{O}_2(\text{a})$ were found to be $\sim 25\%$ of the total O_2 partial pressure at 1 torr (Refs. 16, 23), and so initial $\text{O}_2(\text{X})$ was also known. With known quenching rates for $\text{NF}(\text{b})$ by reactions (xii) and (xiii) (the DF rate was assumed to be slightly less than that of HF; see Section 3.3 for further discussion), we were able to estimate k_{11} and k_{14} . The rate of the reverse of reaction (xi),

k_{-11} , was calculated to be 0.2 k_{11} at 100°C from the known exothermicity of the forward reaction (415 cm^{-1}), and this was included in our iterative procedure.

TABLE III

Generation of $\text{NF}(\text{b}^1\Sigma^+)$

Reaction	Product	Rate Constant ($\text{cm}^3 \text{molecule}^{-1} \text{s}^{-1}$)	Reference No.
(xi) $\text{NF}(\text{a}) + \text{O}_2(\text{a})$	$\text{NF}(\text{b}) + \text{O}_2(\text{X})$	$k_{11} = 6.7 \times 10^{-14}$ $k_{-11} = 1.3 \times 10^{-14}$	This work
Quenching:			
(xii) $\text{NF}(\text{b}) + \text{NF}_2$	$\text{NF}(\text{X}) + \text{NF}_2$	$k_{12} = 3.1 \times 10^{-12}$	28
(xiii) $\text{NF}(\text{b}) + \text{DF}$	$\text{NF}(\text{X}) + \text{DF}$	$k_{13} \sim 1 \times 10^{-12}$	6
(xiv) $\text{NF}(\text{b}) + \text{H}_2\text{O}$	$\text{NF}(\text{X}) + \text{H}_2\text{O}$	$k_{14} = 4.9 \times 10^{-13}$	This work

$\text{NF}(\text{b})$ concentration profiles were generated for given values of k_{11} and k_{14} by numerical integration of the coupled rate equations for all the reactions listed in Tables II and III. By iteration, we were able to reproduce the time averaged experimental [$\text{NF}(\text{b})$] values given in Subsection 2.3.1 with H_2O partial pressures of 1.0 and 0.45 torr. The parameter set determined in the $\text{NF}(\text{a})$ generation calculation (Section 3.1) thus served as a starting point for this extension by inclusion of the reactions in Table III.

Figure 4 shows the resulting curves for $\text{NF}(\text{b})$ generation in the two H_2O pressures. The time averaged value of the lower curve is $4.0 \times 10^{12} \text{ cm}^{-3}$, while that of the upper curve is $6.7 \times 10^{12} \text{ cm}^{-3}$ (cf. [8] and [9] of Subsection 2.3.1).

UNCLASSIFIED
18

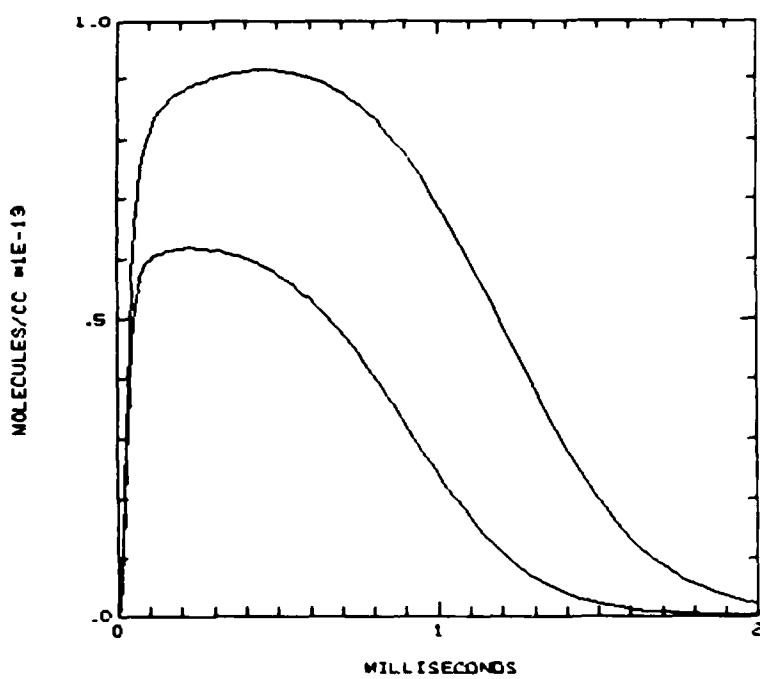


FIGURE 4 - Effect of H₂O on NF(b) generation

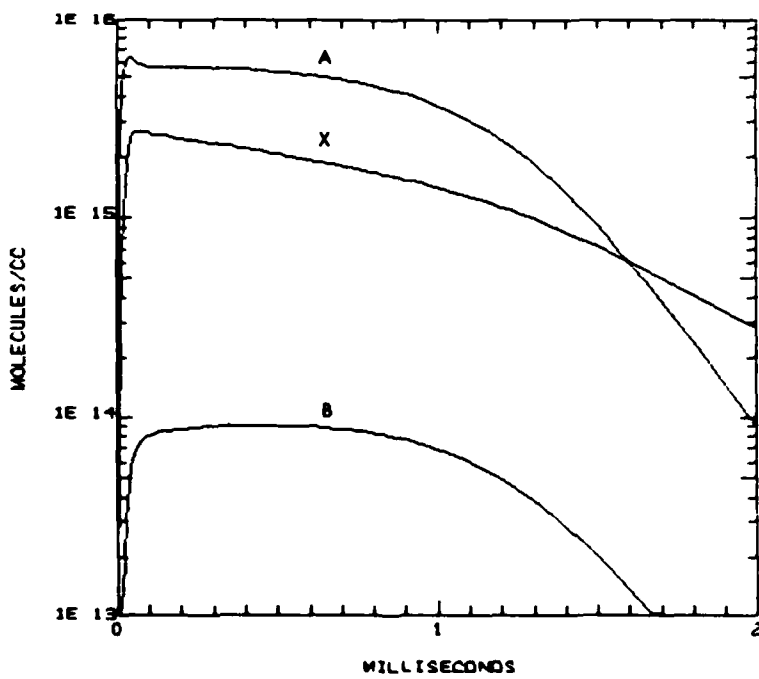


FIGURE 5 - Three electronic states of NF

Figure 5 is a logarithmic plot of the time evolution of the concentrations of all three NF states (X, a and b), under our conditions of maximum $[NF(b)]$, i.e. with 0.45 torr H_2O . It clearly indicates that there is no inversion of population of the b-state with respect to the ground state, $NF(X)$. Even with the rapid ground state disproportionation (reaction (x) of Table II), the $NF(X)$ concentration exceeds that of $NF(b)$ at all times.

Using our set of rate constants for the complete reaction scheme, we were also able to reproduce the HV discharge curve for the time evolution of $NF(b)$ (Fig. 2). In this calculation, only the initial F concentration was varied, and a linear decay function was included to allow for transport of the $NF(b)$ from the viewing region by gas flow. The transport function was

$$g(t) = 1 - vt/x \quad [12]$$

where v is the average gas velocity, t is time, and x is the distance across the viewing aperture (1 cm). The calculated $[NF(b)]$ values were then multiplied by $g(t)$ to give effective observed concentrations. The effect of transport is only significant in the tail of the pulsed signal (Fig. 2). The value of v was allowed to vary to give a least squares fit to the experimental points. The result indicated a gas velocity of 780 cm s^{-1} , which was in excellent agreement with that estimated for our measured pumping speed of 9.2 l. s^{-1} and cross section of 12 cm^2 (770 cm s^{-1}) in the HV discharge cavity. The calculated curve shows a good agreement with the experimental rise time of $[NF(b)]$.

3.3 Accuracy of Rate Constants

It should be noted that rate constants referred to in this section have the units $\text{cm}^3 \text{ molecule}^{-1} \text{ s}^{-1}$. Our calculations of NF a and b quenching rates by H_2O , and the $\text{O}_2(\text{a})/\text{NF}(\text{a})$ pooling rate, are subject to considerable experimental error. The excited state species concentrations were measured to $\pm 20\%$, and partial pressures to between ± 5 and 20% depending on the gas. The literature rate constants given in Tables II and III are quoted at ~ 300 K, whereas our experimental temperature varied between 300 and 400 K, which introduces an error difficult to estimate. An upper limit for the accuracy of the rate constants k_9 , k_{11} and k_{14} given in Tables II and III is therefore about $\pm 50\%$.

Literature values for the quenching rates of $\text{NF}(\text{a},\text{b})$ by DF are not available. However, $\text{NF}(\text{a})$ quenching rates for HCl and HBr are 0.43 and 1.3×10^{-13} respectively (Ref. 28), and the one for HF has an upper limit of 1.7×10^{-13} (Ref. 6). The calculation of $[\text{NF}(\text{a})]$ is not very sensitive to the value used for the DF quenching rate (k_8). We used a value of 1.0×10^{-13} (Table II), but calculations using 1.5 and 0.5×10^{-13} showed variations in average $[\text{NF}(\text{a})]$ of only $\pm 4\%$ respectively. This low sensitivity is due to the fact that DF is a slower quencher of $\text{NF}(\text{a})$ than both NF_2 and H_2O (Table II).

The quenching rate of $\text{NF}(\text{b})$ by HF is 1.7×10^{-12} (Ref. 6). From our experimental observation (Subsection 2.3.1) that $\text{NF}(\text{b})$ emission was reduced by 19% when H_2 replaced D_2 , we infer that DF is a slower quencher of $\text{NF}(\text{b})$ than HF. We used 1.0×10^{-12} for this DF quenching rate (Table III). When the HF quenching rates of $\text{NF}(\text{a},\text{b})$ were used, our calculation reproduced the 19% reduction in average $[\text{NF}(\text{b})]$ observed experimentally, indicating that our DF values are quite reliable.

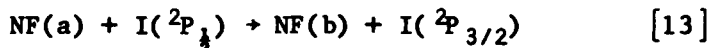
We conclude that our values for the DF quenching rates of $\text{NF}(\text{a},\text{b})$ do not introduce a significant error.

3.4 Rapid Pumping of $\text{NF}(\text{a}^1\Delta)$ for $\text{b}^1\Sigma^+$ Population Inversion

Figure 5 shows that when $\text{O}_2(\text{a}^1\Delta\text{g})$ is used to pump $\text{NF}(\text{a}^1\Delta)$ to produce $\text{NF}(\text{b}^1\Sigma^+)$, only about 1% of the available $\text{NF}(\text{a})$ is found in the b-state at any time. Furthermore, the method is incapable of producing a blue-green laser gain medium since the density of the lower energy state for the 529-nm transition, $\text{NF}(\text{X})$, always exceeds that of the upper state, $\text{NF}(\text{b})$.

This occurs because the $\text{O}_2(\text{a})$ pumping process is slower than the quenching processes (Table III). We have calculated that in order to achieve b-state inversion, a pumping rate constant of $> 10^{-11} \text{ cm}^3 \text{ molecule}^{-1} \text{ s}^{-1}$ is required.

Herbelin and co-workers (Ref. 33) have shown that excited atomic iodine, $\text{I}(\text{2P}_{1/2})$, can also pump $\text{NF}(\text{a})$ to the b-state:

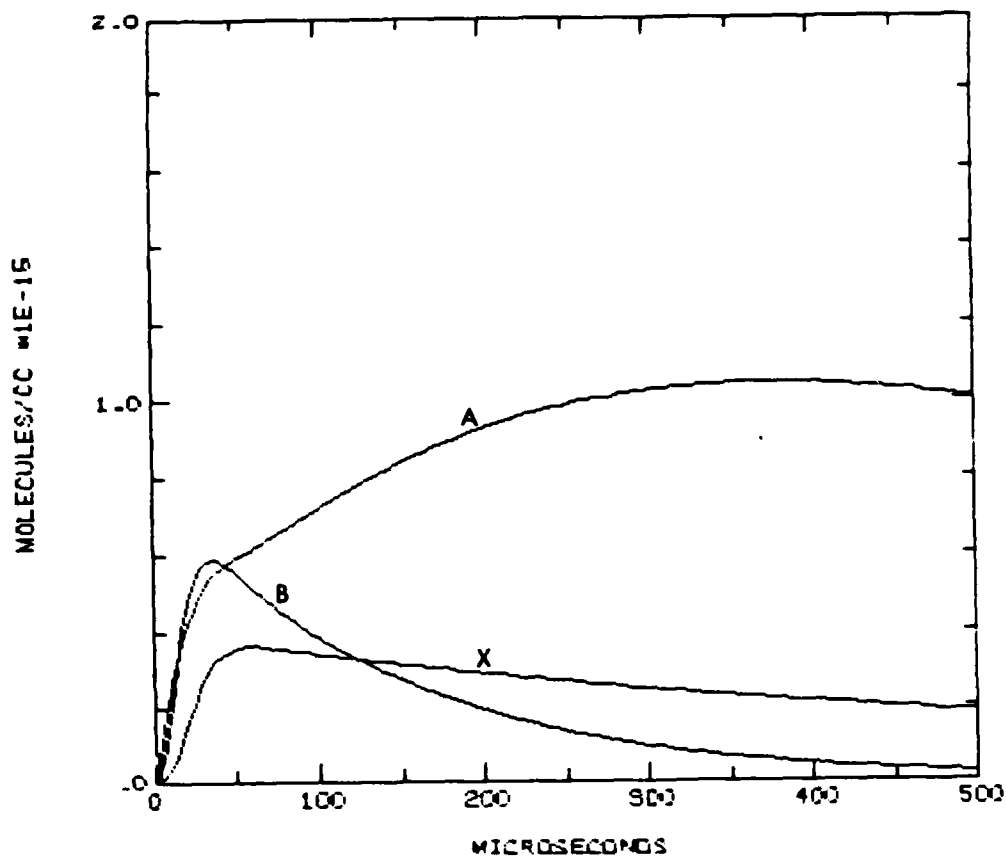


and that the reaction is extremely rapid (rate constant $> 10^{-10} \text{ cm}^3 \text{ molecule}^{-1} \text{ s}^{-1}$).

To demonstrate the potential of reaction [13] to produce the desired population inversion, we have introduced it into our kinetic model as a replacement for the $\text{O}_2(\text{a})$ pumping reaction (x_1) of Table III. We took the forward rate to be $1 \times 10^{-10} \text{ cm}^3 \text{ molecule}^{-1} \text{ s}^{-1}$, and the reverse rate to be 0.6 times this at 100°C, based on an exothermicity of 133 cm^{-1} . With reasonable initial concentrations of F and $\text{I}(\text{2P}_{1/2})$ atoms ($2 \times 10^{15} \text{ cm}^{-3}$), we obtained a maximum $\text{NF}(\text{b})$ density of $\sim 6 \times 10^{14} \text{ cm}^{-3}$. Figure 6 shows the resulting time profiles of the NF states of interest.

UNCLASSIFIED

22

FIGURE 6 - NF pumped by $I(^2P_1)$

Further calculations with higher $I(^2P_1)$ initial densities show that NF(b) densities $> 10^{15} \text{ cm}^{-3}$ should be attainable, providing no significant amounts of IF($X^1\Sigma^+$) are produced in the reaction: IF is a very rapid quencher of NF(b) (Ref. 34).

4.0 CONCLUSIONS

The quenching rates of NF($a^1\Delta$) and NF($b^1\Sigma^+$) by H_2O vapour are:

$$k_{H_2O}^a = 3.7 \times 10^{-13} \quad [14]$$

$$k_{H_2O}^b = 4.9 \times 10^{-13} \quad [15]$$

respectively, and the energy pooling rate between NF($a^1\Delta$) and O₂($a^1\Delta g$) is:

$$k_p = 6.7 \times 10^{-14} \quad [16]$$

with a reverse rate:

$$k_{-p} = 1.3 \times 10^{-14} \quad [17]$$

at about 100°C. The units for the rate constants are cm³ molecule⁻¹ s⁻¹, with approximate error limits $\pm 50\%$.

The NF(a)/O₂(a) reaction is too slow to generate a population inversion of NF($b^1\Sigma^+$) with respect to the ground state. However, b-X population inversion may be possible using the very rapid reaction between NF(a) and I(2P_1). Furthermore, if sufficiently high initial concentrations of I(2P_1) and F atoms ($> 2 \times 10^{15} \text{ cm}^{-3}$) can be generated in a pulsed technique, transient NF($b^1\Sigma^+$) densities in excess of 10^{15} cm^{-3} may be produced within 50 μs of the initiating pulse (see Fig. 6). Such densities would be close to the threshold value required for a blue-green laser at 529 nm operating over a reasonable path length (2 m).

5.0 ACKNOWLEDGEMENTS

Georges Fournier has contributed significantly to this work with many useful discussions, detector construction and calibration, and calculations relating to laser gain conditions. Maurice Verreault and Roger Lambert built the vacuum flow and high-voltage discharge systems, while the former assisted with all the experimental measurements.

UNCLASSIFIED

24

6.0 REFERENCES

1. Fournier, G., *Private Communication*.
2. Tennyson, P.H., Fontijn, A. and Clyne, M.A.A., "Radiative Lifetimes of Metastable States of Free Radicals. I. $NFb^1\Sigma^+$ ", *Chem. Phys.*, Vol. 62, p. 171, 1981.
3. Clyne, M.A.A. and White, I.F., "Electronic Energy Transfer Processes in Fluorine-Containing Radicals: Singlet NF", *Chem. Phys. Lett.*, Vol. 6, p. 465, 1970.
4. Herbelin, J.M. and Cohen, N., "The Chemical Production of Electronically Excited States in the H/NF₂ System", *Chem. Phys. Lett.*, Vol. 20, p. 605, 1973.
5. Herbelin, J.M., "The Role of Electron Spin in the NF Kinetic System", *Chem. Phys. Lett.*, Vol. 42, p. 367, 1976.
6. Kwok, M.A., Herbelin, J.M. and Cohen, N., in "Electronic Transition Lasers II", Wilson, L.E., Suchard, S.N., and Steinfield, J.I., Ed., MIT Press, Boston, 1977.
7. Herbelin, J.M., Spencer, D.J. and Kwok, M.A., "Scale-up of NF(a¹A) Produced by the H₂+NF₂ System in a Subsonic CW Laser Device", *J. Appl. Phys.*, Vol. 48, p. 3050, 1977.
8. Cheah, C.T. and Clyne, M.A.A., "Reactions Forming Electronically Excited Free Radicals. III. Formation of Excited Molecular States in the H+NF₂ Reaction", *J. Photochem.*, Vol. 15, p. 21, 1981.
9. Mallins, R.J. and Setser, D.W., "Rate Constants, Branching Ratios, and Energy Disposal for NF(b,a,X) and HF(v) Formation from the H+NF₂ Reaction", *J. Phys. Chem.*, Vol. 85, p. 1342, 1981.
10. Hack, W. and Horie, O., "Production of Electronically Excited NF Radicals in the System NH₃-F-O₂(¹Δg)", *Chem. Phys. Lett.*, Vol. 82, p. 327, 1981.
11. McDermott, W.E., Pchelkin, N.R., Benard, D.J. and Bousek, R.R., "An Electronic Transition Chemical Laser", *Appl. Phys. Lett.*, Vol. 32, p. 469, 1978.
12. Benard, D.J., McDermott, W.E., Pchelkin, N.R. and Bousek, R.R., "Efficient Operation of a 100-W Transverse-Flow Oxygen-Iodine Chemical Laser", *Appl. Phys. Lett.*, Vol. 34, p. 40, 1979.

UNCLASSIFIED

25

13. Richardson, R.J. and Wiswall, C.E., "Chemically Pumped Iodine Laser", *Appl. Phys. Lett.*, Vol. 35, p. 138, 1979.
14. Richardson, R.J., Wiswall, C.E., Carr, P.A.G., Hovis, F.E. and Lilienfeld, H.V., "An Efficient Singlet Oxygen Generator For Chemically Pumped Iodine Lasers", *J. Appl. Phys.*, Vol. 52, p. 4962, 1981.
15. Bachar, J. and Rosenwaks, S., "An Efficient, Small Scale Chemical Oxygen-Iodine Laser", *Appl. Phys. Lett.*, Vol. 41, p. 16, 1982.
16. Barton, S.A., "Chemical Generation and Deactivation of Oxygen Singlet Delta", DREV R-4310/83, October 1983, UNCLASSIFIED
17. Macdonald, R.G. and Sloan, J.J., "Microscopic V-E Energy Transfer Rates in the HF/NF System", *Chem. Phys. Lett.*, Vol. 61, p. 137, 1979.
18. Badger, R.M., Wright, A.C., and Whitlock, R.F., "Absolute Intensities of the Discrete and Continuous Absorption Bands of Oxygen," *J. Chem. Phys.*, Vol. 43, p. 4345, 1965.
19. Fisk, G.A. and Hays, G.N., "A Study of the 0.634 μm Dimol Emission from Excited Molecular Oxygen", *Chem. Phys. Lett.*, Vol. 79, p. 331, 1981.
20. "JANAF Thermochemical Tables", Stull, D.R. and Prophet, H., Ed., 2nd Edition, U.S. Govt. Printing Office, Washington, D.C., 1971.
21. Collins, R.J. and Husain, D., "Transient Species in the Photolysis of NF_2 ", *J. Photochem.*, Vol. 2, p. 459, 1972/73.
22. Modica, A.P. and Hornig, D.F., "Kinetics of the Thermal Dissociation of N_2F_4 in Shock Waves", *J. Chem. Phys.*, Vol. 49, p. 629, 1968.
23. Barton, S.A., "Estimation of the Concentration of a Photon-Emitting Gas in an Extended Source", DREV R-4290/83, March 1983, UNCLASSIFIED
24. Kuhn, L.P. and Wellman, C., "The Explosive Reaction Between Tetrafluorohydrazine and Hydrogen", *Inorg. Chem.*, Vol. 9, p. 602, 1970.
25. Cheah, C.T., Clyne, M.A.A. and Whitefield, P.D., "Reactions Forming Electronically-Excited Free Radicals. I. Ground-State Reactions Involving NF_2 and NF Radicals", *J.C.S. Faraday II*, Vol. 76, p. 711, 1980.

UNCLASSIFIED

26

26. Davies, P.B. and Temps, F., "Far Infrared Laser Magnetic Resonance Spectrum of NF($a^1\Delta$)", *J. Chem. Phys.*, Vol. 74, p. 6556, 1981.
27. Appelman, E.H. and Clyne, M.A.A., "Elementary Reaction Kinetics of Fluorine Atoms, F0, and NF Free Radicals," *ACS Symposium Series*, No. 66, p. 3, 1978.
28. Cheah, C.T., "Kinetics of Free Radicals Containing Nitrogen and Halogens", Ph.D. Thesis, Queen Mary Coll., Univ. of London, UK, 1980.
29. Wurzberg, E. and Houston, P.L., "The Temperature Dependence of Absolute Rate Constants for the F+H₂ and F+D₂ Reactions", *J. Chem. Phys.*, Vol. 72, p. 4811, 1980.
30. Heidner, R.F., III, Bott, J.F., Gardner, C.E. and Melzer, J.E., "Absolute Rate Coefficients for F+H₂ at T=295-765K," *J. Chem. Phys.*, Vol. 72, p. 4815, 1980.
31. Cohen, N. and Bott, J.F., in "Handbook of Chemical Lasers", Gross, R.W.F. and Bott, J.F., Ed., John Wiley & Sons, New York, 1976.
32. Barton, S.A., "The General Chemical Kinetics Problem: A FORTRAN Program", DREV M-2543/81, April 1981, UNCLASSIFIED
33. Herbelin, J.M., Kwok, M.A. and Spencer, D.J., "Enhancement of NF($B^1\Sigma^+$) by Iodine Laser Pumping", *J. Appl. Phys.*, Vol. 49, p. 3750, 1978.
34. Pritt, A.T., Patel, D. and Benard, D.J., "Iodine Monofluoride Resonant Energy Transfer Chemiluminescence", *Chem. Phys. Lett.*, Vol. 97, p. 471, 1983.

DREV R-4344/84 (UNCLASSIFIED)

Research and Development Branch, DND, Canada.
DREV, P.O. Box 8800, Courcellette, Que. G0A 1R0
"NF(b¹L⁺) from Discharge-Initiated NF(a¹A⁺) and Chemical O₂(a¹A⁺)" by
S.A. Barton and K.D. Foster

Chemically Generated O₂(a¹A⁺) was used to excite NF(a¹A⁺) to NF(b¹L⁺) in a vacuum flow system. NF(a¹A⁺) being produced by the reaction of discharge-generated D atoms with NF^(X) radicals. Maximum concentrations of the NF^(X) a and b states were 5 x 10¹⁴ and 7 x 10¹² cm⁻³ respectively. The latter value is too low to support a blue-green laser based on NF(b¹L⁺).

A complex kinetic model was developed involving 14 known elementary reactions. Using our experimental conditions as input, the coupled rate equations from this model were numerically integrated to yield rate constants for the forward and reverse O₂(a¹A⁺) + NF^(X) reaction (6.7 and 1.3 x 10⁻¹⁴ cm³ molecule⁻¹ s⁻¹ respectively), and for the quenching of NF(a¹A⁺) and NF(b¹L⁺) by H₂O vapour (4 and 5 x 10⁻¹³ cm⁻³ molecule⁻¹ s⁻¹ respectively).

The kinetic model shows that a very fast reaction from NF(a¹A⁺) to NF(b¹L⁺) is required in order to achieve a population inversion between NF(b¹L⁺) and the ground state NF(X). Excited atomic iodine, I(2P_{1/2}), appears to be a better candidate than O₂(a¹A⁺) for generating high densities of NF(b¹L⁺).

DREV R-4344/84 (UNCLASSIFIED)

Research and Development Branch, DND, Canada.
DREV, P.O. Box 8800, Courcellette, Que. G0A 1R0
"NF(b¹L⁺) from Discharge-Initiated NF(a¹A⁺) and Chemical O₂(a¹A⁺)" by
S.A. Barton and K.D. Foster

Chemically Generated O₂(a¹A⁺) was used to excite NF(a¹A⁺) to NF(b¹L⁺) in a vacuum flow system. NF(a¹A⁺) being produced by the reaction of discharge-generated D atoms with NF^(X) radicals. Maximum concentrations of the NF^(X) a and b states were 5 x 10¹⁴ and 7 x 10¹² cm⁻³ respectively. The latter value is too low to support a blue-green laser based on NF(b¹L⁺).

A complex kinetic model was developed involving 14 known elementary reactions. Using our experimental conditions as input, the coupled rate equations from this model were numerically integrated to yield rate constants for the forward and reverse O₂(a¹A⁺) + NF^(X) reaction (6.7 and 1.3 x 10⁻¹⁴ cm³ molecule⁻¹ s⁻¹ respectively), and for the quenching of NF(a¹A⁺) and NF(b¹L⁺) by H₂O vapour (4 and 5 x 10⁻¹³ cm⁻³ molecule⁻¹ s⁻¹ respectively).

The kinetic model shows that a very fast reaction from NF(a¹A⁺) to NF(b¹L⁺) is required in order to achieve a population inversion between NF(b¹L⁺) and the ground state NF(X). Excited atomic iodine, I(2P_{1/2}), appears to be a better candidate than O₂(a¹A⁺) for generating high densities of NF(b¹L⁺).

DREV R-4344/84 (UNCLASSIFIED)

Research and Development Branch, DND, Canada.
DREV, P.O. Box 8800, Courcellette, Que. G0A 1R0
"NF(b¹L⁺) from Discharge-Initiated NF(a¹A⁺) and Chemical O₂(a¹A⁺)" by
S.A. Barton and K.D. Foster

Chemically Generated O₂(a¹A⁺) was used to excite NF(a¹A⁺) to NF(b¹L⁺) in a vacuum flow system. NF(a¹A⁺) being produced by the reaction of discharge-generated D atoms with NF^(X) radicals. Maximum concentrations of the NF^(X) a and b states were 5 x 10¹⁴ and 7 x 10¹² cm⁻³ respectively. The latter value is too low to support a blue-green laser based on NF(b¹L⁺).

A complex kinetic model was developed involving 14 known elementary reactions. Using our experimental conditions as input, the coupled rate equations from this model were numerically integrated to yield rate constants for the forward and reverse O₂(a¹A⁺) + NF^(X) reaction (6.7 and 1.3 x 10⁻¹⁴ cm³ molecule⁻¹ s⁻¹ respectively), and for the quenching of NF(a¹A⁺) and NF(b¹L⁺) by H₂O vapour (4 and 5 x 10⁻¹³ cm⁻³ molecule⁻¹ s⁻¹ respectively).

The kinetic model shows that a very fast reaction from NF(a¹A⁺) to NF(b¹L⁺) is required in order to achieve a population inversion between NF(b¹L⁺) and the ground state NF(X). Excited atomic iodine, I(2P_{1/2}), appears to be a better candidate than O₂(a¹A⁺) for generating high densities of NF(b¹L⁺).

DREV R-4344/84 (UNCLASSIFIED)

Research and Development Branch, DND, Canada.
DREV, P.O. Box 8800, Courcellette, Que. G0A 1R0
"NF(b¹L⁺) from Discharge-Initiated NF(a¹A⁺) and Chemical O₂(a¹A⁺)" by
S.A. Barton and K.D. Foster

Chemically Generated O₂(a¹A⁺) was used to excite NF(a¹A⁺) to NF(b¹L⁺) in a vacuum flow system. NF(a¹A⁺) being produced by the reaction of discharge-generated D atoms with NF^(X) radicals. Maximum concentrations of the NF^(X) a and b states were 5 x 10¹⁴ and 7 x 10¹² cm⁻³ respectively. The latter value is too low to support a blue-green laser based on NF(b¹L⁺).

A complex kinetic model was developed involving 14 known elementary reactions. Using our experimental conditions as input, the coupled rate equations from this model were numerically integrated to yield rate constants for the forward and reverse O₂(a¹A⁺) + NF^(X) reaction (6.7 and 1.3 x 10⁻¹⁴ cm³ molecule⁻¹ s⁻¹ respectively), and for the quenching of NF(a¹A⁺) and NF(b¹L⁺) by H₂O vapour (4 and 5 x 10⁻¹³ cm⁻³ molecule⁻¹ s⁻¹ respectively).

The kinetic model shows that a very fast reaction from NF(a¹A⁺) to NF(b¹L⁺) is required in order to achieve a population inversion between NF(b¹L⁺) and the ground state NF(X). Excited atomic iodine, I(2P_{1/2}), appears to be a better candidate than O₂(a¹A⁺) for generating high densities of NF(b¹L⁺).

A complex kinetic model was developed involving 14 known elementary reactions. Using our experimental conditions as input, the coupled rate equations from this model were numerically integrated to yield rate constants for the forward and reverse O₂(a¹A⁺) + NF^(X) reaction (6.7 and 1.3 x 10⁻¹⁴ cm³ molecule⁻¹ s⁻¹ respectively), and for the quenching of NF(a¹A⁺) and NF(b¹L⁺) by H₂O vapour (4 and 5 x 10⁻¹³ cm⁻³ molecule⁻¹ s⁻¹ respectively).

The kinetic model shows that a very fast reaction from NF(a¹A⁺) to NF(b¹L⁺) is required in order to achieve a population inversion between NF(b¹L⁺) and the ground state NF(X). Excited atomic iodine, I(2P_{1/2}), appears to be a better candidate than O₂(a¹A⁺) for generating high densities of NF(b¹L⁺).

Bureau - Recherche et Développement, MDN, Canada.
CRDV, C.P. 8800, Courcellette, Qué. G0A 1R0

"Formation du NF(b¹D) par la réaction entre NF(a¹A) et O₂(a¹Δg), produit chimiquement", par S.A. Barton et K.D. Foster

Le modèle cinétique montre qu'il faudrait une excitation très rapide de NF(a) à NF(b) afin de réaliser une inversion de population entre NF(b) et l'état fondamental NF(X). L'iode atomique excité I(^{2p}_{1/2}) semble être un meilleur candidat que le O₂(a¹Δg) pour générer de fortes densités de NF(b).

Un modèle cinétique complexe a été développé impliquant 14 réactions élémentaires connues. En utilisant nos valeurs expérimentales, les équations de vitesse couplées ont été intégrées numériquement afin de fournir les constantes de vitesse de la réaction O₂(a¹A) + NF(a) dans les deux directions (6.7 x 10⁻¹⁴ et 1.3 x 10⁻¹⁴ cm³ molécule⁻¹ s⁻¹ pour la réaction inverse). Les constantes de vitesse de la désactivation de NF(a) et NF(b) par H₂O ont aussi été calculées (4 et 5 x 10⁻¹³ cm³ molécule⁻¹ s⁻¹ respectivement).

Le modèle cinétique montre qu'il faudrait une excitation très rapide de NF(a) à NF(b) afin de réaliser une inversion de population entre NF(b) et l'état fondamental NF(X). L'iode atomique excité I(^{2p}_{1/2}) semble être un meilleur candidat que le O₂(a¹Δg) pour générer de fortes densités de NF(b).

Bureau - Recherche et Développement, MDN, Canada.
CRDV, C.P. 8800, Courcellette, Qué. G0A 1R0

"Formation du NF(b¹D) par la réaction entre NF(a¹A) et O₂(a¹Δg), produit chimiquement", par S.A. Barton et K.D. Foster

Le modèle cinétique montre qu'il faudrait une excitation très rapide de NF(a) à NF(b) afin de réaliser une inversion de population entre NF(b) et l'état fondamental NF(X). L'iode atomique excité I(^{2p}_{1/2}) semble être un meilleur candidat que le O₂(a¹Δg) pour générer de fortes densités de NF(b).

Bureau - Recherche et Développement, MDN, Canada.
CRDV, C.P. 8800, Courcellette, Qué. G0A 1R0

"Formation du NF(b¹D) par la réaction entre NF(a¹A) et O₂(a¹Δg), produit chimiquement", par S.A. Barton et K.D. Foster

Le modèle cinétique montre qu'il faudrait une excitation très rapide de NF(a) à NF(b) afin de réaliser une inversion de population entre NF(b) et l'état fondamental NF(X). L'iode atomique excité I(^{2p}_{1/2}) semble être un meilleur candidat que le O₂(a¹Δg) pour générer de fortes densités de NF(b).

Bureau - Recherche et Développement, MDN, Canada.
CRDV, C.P. 8800, Courcellette, Qué. G0A 1R0

"Formation du NF(b¹D) par la réaction entre NF(a¹A) et O₂(a¹Δg), produit par décharge, et O₂(a¹Δg), produit chimiquement", par S.A. Barton et K.D. Foster

Le modèle cinétique montre qu'il faudrait une excitation très rapide de NF(a) à NF(b) dans un système d'écoulement sous vide. Du NF(a) a alors été formé par la réaction engendrée par une décharge d'atomes D avec des radicaux NF₂. Les concentrations maximales de NF déterminées dans les états a et b sont respectivement 5 x 10⁻¹⁴ et 7 x 10⁻¹² cm⁻³. Cette dernière concentration est trop faible pour supporter une action laser basée sur le NF(b¹D) dans la région bleu-vert.

Un modèle cinétique complexe a été développé impliquant 14 réactions élémentaires connues. En utilisant nos valeurs expérimentales, les équations de vitesse couplées ont été intégrées numériquement afin de fournir les constantes de vitesse de la réaction O₂(a¹A) + NF(a) dans les deux directions (6.7 x 10⁻¹⁴ et 1.3 x 10⁻¹⁴ cm³ molécule⁻¹ s⁻¹ pour la réaction inverse). Les constantes de vitesse de la désactivation de NF(a) et NF(b) par H₂O ont aussi été calculées (4 et 5 x 10⁻¹³ cm³ molécule⁻¹ s⁻¹ respectivement).

Le modèle cinétique montre qu'il faudrait une excitation très rapide de NF(a) à NF(b) afin de réaliser une inversion de population entre NF(b) et l'état fondamental NF(X). L'iode atomique excité I(^{2p}_{1/2}) semble être un meilleur candidat que le O₂(a¹Δg) pour générer de fortes densités de NF(b).

Bureau - Recherche et Développement, MDN, Canada.
CRDV, C.P. 8800, Courcellette, Qué. G0A 1R0

"Formation du NF(b¹D) par la réaction entre NF(a¹A) et O₂(a¹Δg), produit par décharge, et O₂(a¹Δg), produit chimiquement", par S.A. Barton et K.D. Foster

Le modèle cinétique montre qu'il faudrait une excitation très rapide de NF(a) à NF(b) dans un système d'écoulement sous vide. Du NF(a) a alors été formé par la réaction engendrée par une décharge d'atomes D avec des radicaux NF₂. Les concentrations maximales de NF déterminées dans les états a et b sont respectivement 5 x 10⁻¹⁴ et 7 x 10⁻¹² cm⁻³. Cette dernière concentration est trop faible pour supporter une action laser basée sur le NF(b¹D) dans la région bleu-vert.

Un modèle cinétique complexe a été développé impliquant 14 réactions élémentaires connues. En utilisant nos valeurs expérimentales, les équations de vitesse couplées ont été intégrées numériquement afin de fournir les constantes de vitesse de la réaction O₂(a¹A) + NF(a) dans les deux directions (6.7 x 10⁻¹⁴ et 1.3 x 10⁻¹⁴ cm³ molécule⁻¹ s⁻¹ pour la réaction inverse). Les constantes de vitesse de la désactivation de NF(a) et NF(b) par H₂O ont aussi été calculées (4 et 5 x 10⁻¹³ cm³ molécule⁻¹ s⁻¹ respectivement).

Le modèle cinétique montre qu'il faudrait une excitation très rapide de NF(a) à NF(b) afin de réaliser une inversion de population entre NF(b) et l'état fondamental NF(X). L'iode atomique excité I(^{2p}_{1/2}) semble être un meilleur candidat que le O₂(a¹Δg) pour générer de fortes densités de NF(b).

END

FILMED

4-85

DTIC